Journal of the Serbian Chemical Society
JSCS-info@shd.org.rs • www.shd.org.rs/JSCS

ACCEPTED MANUSCRIPT

Journal of the Serbian Chemical Society
JSCS-info@shd.org.rs • www.shd.org.rs/JSCS
J. Serb. Chem. Soc. **00(0)** 1-25 (2024)
JSCS–12720
Original scientific paper
Published DD MM, 2024

Ultrasonic and spectroscopic investigations of molecular interactions in binary mixture of PEG-400 and DMSO at different temperatures

MONIKA DHIMAN[1], ARUN UPMANYU[1]*, DEVINDER PAL SINGH[2] and KAILASH CHANDRA JUGLAN[3]

[1]*Chitkara University Institute of Engineering and Technology, Chitkara University, Punjab, 140401, India,* [2]*Acoustics Research Center, Mississauga, L5A 1Y7, Ontario, Canada, and* [3]*Department of Physics, Lovely Faculty of Technology and Sciences, Lovely Professional University, Punjab, India*

(Received 7 December 2023; revised 22 January 2024; accepted 2 June 2024)

Abstract: In the present study, the ultrasonic velocity and density data for the binary mixture of Polyethylene Glycol (PEG)-400 and Dimethyl Sulfoxide (DMSO), at various concentrations and different temperatures (T = 288.15 K, 298.15 K and 308.15 K), have been measured and further utilized to determine several physical parameters such as adiabatic and isothermal compressibility, intermolecular free length, internal pressure, and free volume. Excess values of these parameters have also been computed and fitted with the Redlich-Kister (R-K) polynomial equation. The nature, type, and strength of intermolecular interactions present within the PEG-400 + DMSO mixture have been explained based on the sign and magnitude of excess values. Furthermore, partial molar volumes, excess partial molar volumes, apparent molar volumes, and apparent molar volumes at infinite dilution have also been determined to investigate the solute-solvent interactions. Various mixing rules such as the ideal mixing rule (U_{im}), Nomoto relation (U_N), impedance dependence relation (U_Z), Junjie relation (U_J), Van Deal-Vangeel relation (U_V) and collision factor theory (U_{CFT}) are employed to compute the ultrasonic velocity and compared with the experimental one. Among these relations, the Nomoto and Junjie relations are found to be most suitable for the given mixture. In addition to it, the present system has also been examined using Fourier Transform Infra-Red (FTIR) and Ultraviolet-visible (UV-Vis) spectroscopic techniques. The change in intensity and shift in peak position in the FTIR and UV-vis spectra of the PEG-400 + DMSO mixture are utilized to confirm the intermolecular hydrogen bonding in the given system.

* Corresponding author. E-mail: arun.upmanyu@chitkara.edu.in
https://doi.org/10.2298/JSC231207058D

Keywords: research development; industry; sustainable development; polyethylene glycol; Fourier transform infra-red (FTIR); ultraviolet-visible (UV-Vis).

INTRODUCTION

In recent years, several researchers have contributed to synthesizing and characterizing significant industrial materials and tuning them to specific applications.[1–5] In such chemical synthesis, the emission of sulphur dioxide (SO_2) is a serious concern that affects the health and environmental sectors.[3–5] Therefore, various processes/techniques have been developed over time to remove SO_2 from industrial products, a process called desulphurisation.[6–8] Dimethyl sulfoxide (DMSO) is a widely used organic solvent for removing SO_2 due to its high solubility for sulphur-containing compounds. However, the high freezing point (18ºC) of DMSO causes problems to use it in the low-temperature range. Adding another biocompatible Polyethylene Glycol (PEG)-400 into DMSO will overcome this limitation. The other advantages of the PEG-400 + DMSO mixture are its relatively low toxicity and better solubility than virgin DMSO. Furthermore, it can be easily recovered and reused in chemical processes.

A comprehensive review of the literature[6,9–12] reveals that most of the investigations into the PEG-400 and DMSO systems are made to understand their behaviour towards desulphurisation, whereas only limited work is available to explore the nature and strength of inter- and intra-molecular interactions prevalent within the system based on the ultrasonic velocity, density, and viscosity. Zhang *et al.*[6] also measured the density of the PEG-400 + DMSO mixture at different concentrations and temperatures. To compare the reported density data with the present data at mutual temperatures (298.15 K and 308.15 K), we have generated the fitting equation for density measured in this work given below;

$$d^* = Y_0 + A \exp(R_0 . X_1) \quad (1)$$

Where Y_0, A and R_0 are the arbitrary constants and their values at (a) T=298.15 K are; Y_0 = 1.1216, A = -0.0244 and R_0= -4.8551;(b) T=308.15 K are; Y_0= 1.1139, A = -0.0258 and R_0= -4.0890.

Thereafter, Equation (1) was used to compute the density (d^*) at the same mole fractions as reported in a research paper by Zhang *et al.*[6] The correlation of measured density and reported in literature[6] along with absolute average percentage deviation (AAPD) at 298.15 K and 308.15 K are given in Table S1 (Supporting information). The perusal of Table S1 indicates that the AAPD is 0.1550 and 0.1488 at 298.15 K and 308.15 K respectively. For a better understanding, the density data obtained in the present study and literature,[6] along with the fitting line, are given in Figure S1 and Figure S2 (Supporting information). Additionally, the density values of current measurement (using Equation (1)) and literature[6] at the same mole fractions are presented in Figure S4 and Figure S5. The

probable reason for the deviation can be; (i) Zhang *et al.*[6] performed the pre-processing (drying over molecular sieves (type 4A) and decompression filtration by vacuum pump), before density measurement of the materials, whereas in the present work, these materials are used as such without any further purification; (ii) Additionally, we have measured the density using more sophisticated DSA 5000 M interferometer, with density accuracy of 0.000001 g.cm^{-3}; whereas, Zhang *et al.*[6] measured density using bicapillary pycnometer.

Moreover, there are several techniques such as infrared (IR) spectroscopy, nuclear magnetic resonance (NMR) spectroscopy, UV-visible spectroscopy, X-ray crystallography, Surface plasmon resonance (SPR), Isothermal titration calorimetry (ITC), fluorescence resonance energy transfer (FRET) technique, ultrasonic, volumetric, and refractometric techniques are available to investigate different types of molecular interactions in the solid/liquid systems. A literature survey[13–18] reveals that the ultrasonic technique is widely accepted to study molecular interactions for liquid systems due to its unique features like its non-destructive nature, real-time monitoring, versatility, high sensitivity, and non-invasiveness. The ultrasonic technique involves measuring the speed and attenuation of ultrasonic waves as they pass through a liquid system. The speed of the ultrasonic wave is affected by the density and compressibility of the liquid mixture, while the attenuation is affected by the viscosity and molecular interactions present in the system. By analysing the changes in speed and attenuation of the ultrasonic waves, it is possible to obtain information about the nature, type, and strength of interactions among the constituent molecules of the mixture. The speed of sound in conjunction with density can be further employed to compute several important thermodynamical parameters such as acoustic impedance, adiabatic compressibility, intermolecular free length, internal pressure, free volume, etc., which are generally difficult to determine experimentally. The concentration and temperature dependence of these parameters also provide useful information about inter and intra-molecular interactions prevalent in the system. Other useful techniques to study the molecular interactions in liquid systems are FTIR, UV, and NMR spectroscopy.[19–21] These techniques rely on the interaction of electromagnetic radiation with the molecules in a sample. The absorption, emission, or scattering of electromagnetic radiation by the sample is measured. The obtained data provides information about the sample's molecular structure and interactions. At present, ultrasonic and spectroscopic techniques are regularly used to investigate the molecular interactions in organic liquids, polymers, polymer blends, ionic liquids, and liquid crystals.[22–24]

In the present work, ultrasonic velocity and density values are measured for PEG-400 + DMSO at different mole fractions and temperatures (288.15 K, 298.15 K, and 308.15 K). The measured data is utilized to compute several important thermodynamical parameters such as adiabatic and isothermal compressibility,

intermolecular free length, internal pressure, free volume, and their excess values. FTIR and UV-Vis spectroscopic investigation has also been taken to explore the molecular interactions in the system under study. The variations in sign and magnitude of excess parameters, with changes in concentration and temperature, have been used to complement/supplement the information obtained via other investigative techniques about the nature, type, and strength of molecular interactions prevalent in the system under study.

EXPERIMENTAL

Materials

Polyethylene Glycol (PEG) and DMSO with molar masses of 400 $g.mol^{-1}$ and 78.14 $g.mol^{-1}$, respectively, and purity ≥ 99% were acquired from Loba Chemie Pvt. Ltd., India. The chemicals were used without any further purification for the measurement of ultrasonic velocity (U) and density (d).

Measurement procedure of ultrasonic velocity (U) and density (d)

The ultrasonic velocity (*U*) and density (*d*) of the pure PEG-400, DMSO, and their mixture at different mole fractions were measured at the three different temperatures (T = 288.15 K, 298.15 K, and 308.15 K) using Anton Paar DSA 5000M densimeter which worked at 3MHZ. The inbuilt Peltier-thermostat of the densimeter controlled the temperature automatically and the working temperature was estimated accurately up to ±0.01K. The *U* and *d* were measured by infusing the sample with a syringe inside the instrument. The instrument can measure density with an accuracy of 0.000001 $g.cm^{-3}$ and ultrasonic velocity with an accuracy of 0.01 ms^{-1}. For density measurement, the apparatus was calibrated with doubly distilled degassed water, and with dry air at atmospheric pressure. The repeatability is obtained with triplicate measurements on the same sample maintained inside the densimeter at a constant temperature at different times during the course of present measurements. The density and speed of sound measurements both had experimental uncertainties below 0.0005 $g \cdot m^{-3}$ and 1.0 $m \cdot s^{-1}$ respectively. Binary mixtures were prepared by mass, using an analytical balance with a precision of 0.0001 g (Denver Instrument APX-200). The mole fraction of each mixture was obtained with an accuracy of 0.0001 from the measured masses of the components. The measured values of *U* and *d* of pure components had been compared with literature data and are reported in Table I. The perusal of Table I indicates that the percentage deviation between experimental and literature values of density and ultrasonic velocity for PEG-400 and DMSO is less than 0.3% at all temperatures. The comparisons between experimental and literature densities and ultrasonic velocity are presented in Figure 1(a-d).

Table I. Experimental and literature values of ultrasonic velocity (U) and density (d) of pure PEG-400 and DMSO[a].

Component	T / K	U (m/s)			d (g/cm^3)		
		Expt.	Lit.	Modulus of % deviation	Expt.	Lit.	Modulus of % deviation
PEG-400	288.15	1629.30	-		1.13031	1.13126[25]	0.084
	298.15	1595.16	1592.8[26]	0.146	1.12199	1.1226[6]	0.060
			1595.03[27]	0.008		1.12225[25]	0.023
			1593.01[28]	0.135		1.12239[26]	0.036
			1593.20[29]	0.123		1.122308[27]	0.028
						1.12230[28]	0.028
	308.15	1561.90	1558.9[30]	0.190	1.11373	1.1139[6]	0.021
			1564.4[26]	0.162		1.1128[30]	0.081
			1561.58[27]	0.020		1.11433[26]	0.054
			1559.50[28]	0.153		1.11487[27]	0.103
			1558.99[29]	0.186		1.11489[28]	0.104
DMSO	288.15	1524.25	-		1.10574	-	
	298.15	1490.12	1493[31]	0.193	1.09572	1.0958[6]	0.013
			1484.8[32]	0.356		1.0952[32]	0.045
			1489.2 [33]	0.062		1.0957[19]	0.000
			1485.10[34]	0.338		1.0954[35]	0.026
			1484[36]	0.412		1.09729[33]	0.144
			1485.12[37]	0.336		1.095387[34]	0.030
			1485.5[38]	0.308		1.09537[39]	0.032
			1487[40]	0.210		1.09562[41]	0.009
			1485.12[42]	0.336		1.09537[43]	0.032
			1484.29[44]	0.392		1.09527[45]	0.041
	308.15	1456.54	1450.9[32]	0.385	1.08720	1.08070[46]	0.598
			1451.3[34]	0.357		1.0852[32]	0.181
			1451.6[39]	0.337		1.08548[10]	0.158
			1451.28[34]	0.361		1.0857[19]	0.136
						1.085348[34]	0.170
						1.08550[47]	0.156
						1.0856[48]	0.143
						1.0839[6]	0.304

[a]The standard uncertainties (u) are $u(T)$= 0.01 K, $u(d)$= 0.5 kgm^{-3}, $u(U)$= 1.0 ms^{-1}.

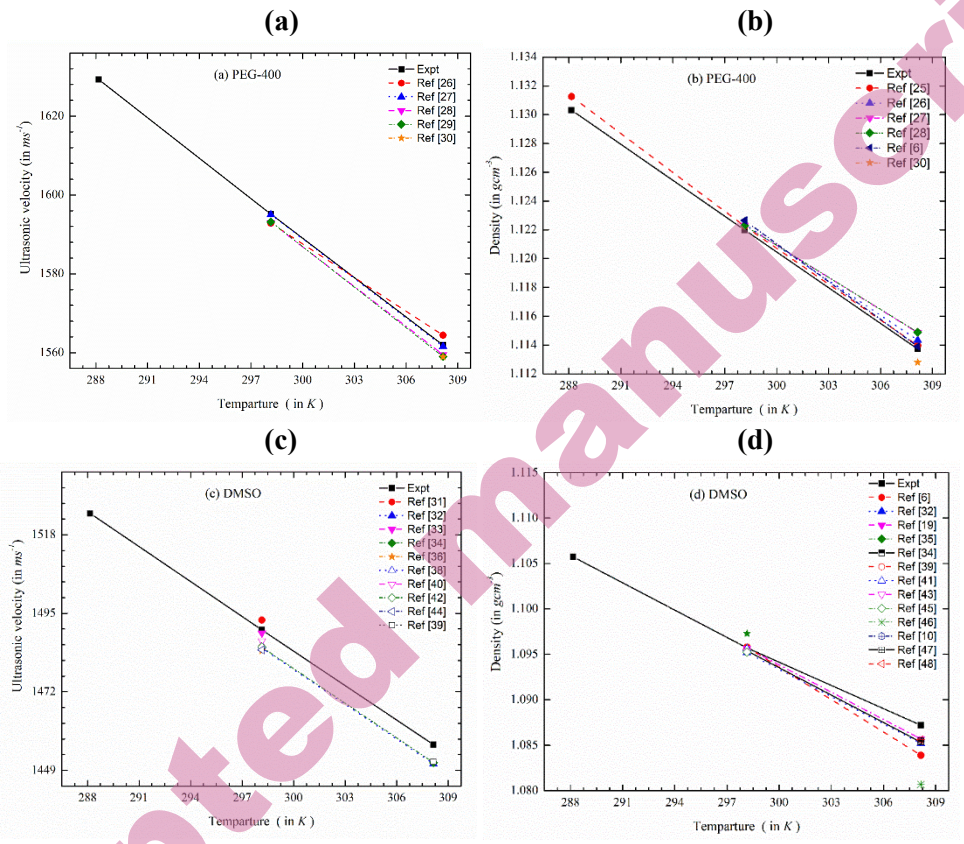

Fig. 1. The plot of experimental and literature values: **(a)** of ultrasonic velocity of PEG-400 at 288.15 K, 298.15 K, and 308.15 K; **(b)** of density of PEG-400 at 288.15 K, 298.15 K, and 308.15 K; **(c)** for the ultrasonic velocity of DMSO at 288.15 K, 298.15 K, and 308.15 K; **(d)** values for the density of DMSO at 288.15 K, 298.15 K, and 308.15 K. The solid and dotted lines are a guide for the eye.

FTIR and UV-Vis Spectroscopy

The FTIR spectrum for the mixture under study was recorded on sophisticated FTIR (Bruker, Model - Eco AR Alpha II) equipped with OPUS software. The spectrometer possessed auto-align energy optimization, dynamically aligned with and RockSolid™ cube corner interferometer and Temperature-controlled DLaTGS-detector. Data were recorded in the spectral range of 400–4,000 cm^{-1} at 4 cm^{-1} spectral resolution with standard KBr beam splitter possessing precision and accuracy of 0.05 cm^{-1} @ 1576 cm^{-1} and <0.0006 cm^{-1} @ 1576 cm^{-1}. A baseline correction was made for the spectra recorded in the air. For each measurement 10 µL solution was used with sample layer thickness typically less than 2 µm. All these measurements were performed at room temperature and atmospheric pressure.

The UV-Vis spectrum for the mixture was recorded on Systronics (India) PC-Based Double Beam UV-Vis Spectrophotometer-2202. The Spectrophotometer was equipped with Modified Czerny-Turner Monochromator geometry for better aberration correction,

holographic diffraction grating with 1200 lines/mm blazed at 250 nm, and advanced beam technology with PC-controlled settings. The apparatus operates in the wavelength range from 200 nm to 1100 nm at a resolution of 0.1 nm with an accuracy of ±0.5 nm. In the present case, DMSO is used to make the baseline correction for the spectra.

Theoretical Formulation

The experimentally measured data for U and d have been used to compute some physical parameters such as adiabatic compressibility (K_s), isothermal compressibility (K_T), intermolecular free length (L_f), free volume (V_f), and internal pressure (P_i) by employing following standard formulations as reported in the literature:[13]

$$K_s = \frac{1}{U^2 d} \tag{2}$$

$$K_T = \frac{1.71 \times 10^{-3}}{T^{4/9} U^2 d^{4/3}} \tag{3}$$

$$L_f = \frac{2V_a}{Y_s} \tag{4}$$

where $Y_S = (36\pi N V_0^2)^{1/3}$ is the molar surface area, N is Avogadro's number, and $V_o = V\text{-}V_a$.

where V is the molar volume, Va is the available volume at any given temperature, and V_o is the molar volume of liquid at absolute zero temperature.

The internal pressure (P_i) is a measure of the strength of forces between the molecules and is obtained by using the following relation:

$$P_i = \frac{T\alpha}{K_T} \tag{5}$$

Where T is temperature, K_T is isothermal compressibility, and volume expansivity (α) is given by $\alpha = (0.0191 \times K_T)^{1/4}$.

Another important parameter free volume (V_f), which is the average volume of free space between the two neighbouring molecules is given below:

$$V_f = \frac{RT}{P+P_i} \tag{6}$$

Where P is external pressure, which is negligible as compared to internal pressure (P_i), R = universal gas constant, and T = Temperature.

Theoretical evaluation of ultrasonic velocity (U) has been done using various mixing rules viz., ideal mixing rule (U_{im}), Nomoto relation (U_N), impedance dependence relation (U_Z), Junjie relation (U_J), Van Deal-Vangeel relation (U_V), and collision factor theory (U_{CFT}). The mathematical formulations for these relations are given below:[13]

The ideal mixing relation (U_{im}) uses the speed of sound of pure components along with mole fraction to predict the ultrasonic velocity of the mixture, as:

$$U_{IM} = \sum_i^2 X_i U_i \tag{7}$$

where Xi and Ui (i =1,2) are the mole fraction and sound velocity of pure components, respectively.

Nomoto relation (U_N) based on the assumption of no volume change on mixing, is given as:

$$U_N = \left\{\frac{(X_1R_1 + X_2R_2)}{X_1V_1 + X_2V_2}\right\}^3 \tag{8}$$

Where V_1 and V_2 are the molar volumes and R_1 and R_2 are the molar sound velocity values of the pure components in the binary mixture.

The standard form of impedance dependence relation (U_Z) to predict ultrasonic velocity is:

$$U_Z = \frac{X_1Z_1+X_2Z_2}{X_1d_1+X_2d_2} \quad (9)$$

where (X_1, X_2), (Z_1, Z_2) and (d_1, d_2) are, respectively, the mole fraction, acoustic impedance, and density values of pure components in a binary mixture.

Junjie relation (U_J) predicts ultrasonic velocity using mole fractions X_1 and X_2, molar masses M_1 and M_2, molar volumes V_1 and V_2, density d_1, and $d_2$and ultrasonic speed U_1 and U_2 of pure components:[49]

$$U_J = \frac{(X_1V_1+X_2V_2)}{\sqrt{(X_1M_1+X_2M_2)\left(\frac{X_1V_1}{d_1U_1^2}\right)+\left(\frac{X_2V_2}{d_2U_2^2}\right)}} \quad (10)$$

Van Deal and Vangeel (U_V) modified the ideal mixing relation using molar weight M_1 and M_2 of pure components;[13]

$$U_V = (X_1M_1 + X_2M_2)\left(\frac{X_1}{M_1U_1^2} + \frac{X_2}{M_2U_2^2}\right)^{-1/2} \quad (11)$$

The collision factor theory (U_{CFT}) is based on the concept of collisions taking place amongst liquid molecules and the free space available between them. It provides an expression for the calculation of ultrasonic velocities in a binary mixture, as given below:[13]

$$U_{CFT} = U_\infty\,(X_1S_1 + X_2S_2)\left\{\frac{(X_1B_1+X_2B_2)}{V}\right\} \quad (12)$$

where U_∞ is the limiting value of sound velocity for liquids, which is taken as 1600 ms^{-1}. S_1 and S_2 are collision factors. B_1 and B_2 are geometrical volumes per mole of solute and solvent respectively.

RESULTS AND DISCUSSION

Acoustical parameters and molecular interactions

Experimentally measured ultrasonic velocity (U) and density (d) data for PEG-400 + DMSO binary mixture at various concentrations and temperatures is reported in Table II. Therein, the obtained results are presented as a function of the mole fraction (X_1) of PEG-400 at different temperatures (T= 288.15 K, 298.15 K and 308.15 K).

Using the experimentally measured U and d values, some acoustical and thermodynamical parameters viz., K_s, K_T, L_f, V_f, and P_i, have been determined. These parameters are reported in Table III. Several researchers have pointed out that acoustical and thermodynamical parameters are important tools to explore the nature and strength of molecular interactions in a liquid system.[50–52] Keeping this in view, we have computed the excess values of these acoustical and thermodynamical parameters using a standard relation as given below:

$$A^{Excess} = A^{Expt} - (A_1X_1 + A_2X_2) \quad (13)$$

Table II. Measured values of ultrasonic velocity (U) and density (d) of PEG-400 (X_1) + DMSO (X_2) at different temperatures.

X_1	288.15 K		298.15 K		308.15 K	
	U (ms^{-1})	d (gcm^{-3})	U (ms^{-1})	d (gcm^{-3})	U (ms^{-1})	d (gcm^{-3})
0	1524.25	1.10574	1490.12	1.09572	1456.54	1.08720
0.0477	1564.03	1.11383	1522.6	1.10408	1489.42	1.09452
0.0790	1569.29	1.11716	1534.37	1.10604	1497.3	1.09549
0.1178	1574.43	1.11877	1547.78	1.10785	1513.44	1.09787
0.1668	1587.41	1.12024	1559.49	1.10936	1529.19	1.09934
0.2310	1598.23	1.12464	1567.88	1.11288	1539.9	1.10375
0.3185	1612.76	1.12614	1579.28	1.11712	1548.13	1.10771
0.4448	1618.22	1.12792	1583.57	1.11870	1550.07	1.11007
0.5516	1621.16	1.12855	1586.64	1.11957	1553.20	1.11104
0.6431	1623.25	1.12900	1588.84	1.12019	1555.44	1.11173
0.8278	1626.71	1.12975	1592.45	1.12122	1559.13	1.11287
1	1629.30	1.13031	1595.16	1.12199	1561.9	1.11373

Where A represents K_s, K_T, L_f, V_f, and P_i. A^{Excess} and A^{Expt} are the excess and experimental values of A. X_1 and X_2 are the mole fractions of solute and solvent respectively.

The excess values of all these parameters as a function of the mole fraction (X_1) of PEG-400 are plotted in Fig. 2 to Fig. 6 at different temperatures. These excess values are also fitted with Redlich-Kister (R-K)[11] type polynomial equation given below:

$$\Delta Y = X_1 X_2 \sum_{K=1}^{n} A_K \, (2X_1 - 1)^{K-1} \tag{14}$$

where ΔY is the excess parameter to be fitted with the R-K polynomial equation, and A_K is the fitting parameter. The number of fitting parameters is optimized by using F-test.[53] The standard deviations (σ) are computed using the relation:

$$\sigma(\Delta Y) = \left[\frac{\sum(\Delta Y_{expt} - \Delta Y_{cal})}{N-n}\right]^{1/2} \tag{15}$$

where N is the total number of mole fractions and n is the number of fitting parameters. ΔY_{expt} and ΔY_{cal} are the experimental and calculated values of excess parameters. The computed values of R-K coefficients and standard deviations (σ) are reported in Table IV.

Table III. Acoustical parameters viz., free volume (V_f), adiabatic compressibility (K_s), isothermal compressibility (K_T), intermolecular free length (L_f), and internal pressure (P_i) for PEG-400 + DMSO at different temperatures.

X_1	$V_f \times 10^6$ (m^3mol^{-1})	$K_s \times 10^{-10}$ (Pa^{-1})	$K_T \times 10^{-10}$ (Pa^{-1})	L_f (pm)	P_i (MPa)
			T = 288.15 K		
0	4.327(± 0.004)	3.893(± 0.005)	5.194(± 0.007)	39.84(± 0.042)	553.7(± 0.006)
0.0477	4.133(± 0.004)	3.670(± 0.005)	4.886(± 0.007)	38.69(± 0.035)	579.7(± 0.006)
0.0790	4.100(± 0.004)	3.635(± 0.005)	4.834(± 0.006)	38.50(± 0.034)	584.3(± 0.006)
0.1178	4.074(± 0.004)	3.606(± 0.005)	4.793(± 0.006)	38.35(± 0.034)	588.1(± 0.006)
0.1668	4.019(± 0.004)	3.543(± 0.005)	4.707(± 0.006)	38.01(± 0.032)	596.1(± 0.006)
0.2310	3.962(± 0.004)	3.481(± 0.005)	4.619(± 0.006)	37.68(± 0.030)	604.6(± 0.006)
0.3185	3.904(± 0.004)	3.414(± 0.004)	4.528(± 0.006)	37.31(± 0.029)	613.7(± 0.006)
0.4448	3.878(± 0.003)	3.386(± 0.004)	4.488(± 0.006)	37.16(± 0.028)	617.8(± 0.006)
0.5516	3.865(± 0.003)	3.372(± 0.004)	4.468(± 0.006)	37.08(± 0.028)	619.8(± 0.006)
0.6431	3.856(± 0.003)	3.361(± 0.004)	4.454(± 0.006)	37.02(± 0.027)	621.3(± 0.006)
0.8278	3.841(± 0.003)	3.345(± 0.004)	4.432(± 0.006)	36.93(± 0.027)	623.7(± 0.006)
1	3.830(± 0.003)	3.333(± 0.004)	4.415(± 0.006)	36.86(± 0.027)	625.5(± 0.006)
			T = 298.15 K		
0	4.466(± 0.004)	4.110(± 0.006)	5.418(± 0.008)	41.70(± 0.050)	555.0(± 0.006)
0.0477	4.291(± 0.004)	3.907(± 0.005)	5.137(± 0.007)	40.65(± 0.043)	577.6(± 0.006)
0.0790	4.235(± 0.004)	3.840(± 0.005)	5.047(± 0.007)	40.31(± 0.041)	585.4(± 0.006)
0.1178	4.173(± 0.004)	3.768(± 0.005)	4.949(± 0.007)	39.93(± 0.039)	594.0(± 0.006)
0.1668	4.120(± 0.004)	3.706(± 0.005)	4.866(± 0.007)	39.60(± 0.037)	601.6(± 0.006)
0.2310	4.074(± 0.004)	3.655(± 0.005)	4.794(± 0.006)	39.32(± 0.036)	608.4(± 0.006)
0.3185	4.015(± 0.004)	3.589(± 0.005)	4.701(± 0.006)	38.97(± 0.034)	617.4(± 0.006)
0.4448	3.993(± 0.004)	3.565(± 0.005)	4.667(± 0.006)	38.83(± 0.033)	620.8(± 0.006)
0.5516	3.978(± 0.004)	3.548(± 0.005)	4.644(± 0.006)	38.74(± 0.033)	623.1(± 0.006)
0.6431	3.968(± 0.004)	3.536(± 0.005)	4.628(± 0.006)	38.68(± 0.032)	624.7(± 0.006)
0.8278	3.951(± 0.004)	3.517(± 0.005)	4.601(± 0.006)	38.57(± 0.032)	627.4(± 0.006)
1	3.938(± 0.004)	3.503(± 0.005)	4.581(± 0.006)	38.49(± 0.031)	629.4(± 0.006)
			T = 308.15 K		
0	4.607(± 0.004)	4.336(± 0.006)	5.647(± 0.008)	43.61(± 0.059)	556.1(± 0.006)
0.0477	4.426(± 0.004)	4.119(± 0.006)	5.352(± 0.008)	42.50(± 0.051)	578.9(± 0.006)
0.0790	4.387(± 0.004)	4.072(± 0.006)	5.290(± 0.007)	42.26(± 0.049)	584.0(± 0.006)
0.1178	4.307(± 0.004)	3.977(± 0.006)	5.163(± 0.007)	41.76(± 0.046)	594.8(± 0.006)
0.1668	4.235(± 0.004)	3.890(± 0.005)	5.048(± 0.007)	41.31(± 0.043)	604.9(± 0.006)
0.2310	4.174(± 0.004)	3.821(± 0.005)	4.951(± 0.007)	40.94(± 0.041)	613.7(± 0.006)
0.3185	4.126(± 0.004)	3.767(± 0.005)	4.876(± 0.007)	40.65(± 0.039)	620.9(± 0.006)
0.4448	4.110(± 0.004)	3.749(± 0.005)	4.850(± 0.007)	40.55(± 0.039)	623.4(± 0.006)
0.5516	4.094(± 0.004)	3.731(± 0.005)	4.756(± 0.007)	40.45(± 0.038)	632.6(± 0.006)
0.6431	4.083(± 0.004)	3.718(± 0.005)	4.807(± 0.007)	40.38(± 0.038)	627.5(± 0.006)
0.8278	4.064(± 0.004)	3.696(± 0.005)	4.777(± 0.006)	40.27(± 0.037)	630.4(± 0.006)
1	4.050(± 0.004)	3.681(± 0.005)	4.756(± 0.006)	40.18(± 0.037)	632.6(± 0.006)

[a]The standard uncertainties (u) are $u(T)$= 0.01 K, $u(d)$= 0.5 kgm^{-3}, $u(U)$= 1.0 ms^{-1}.

Table IV. Coefficients of Redlich – Kister (R-K) equation and standard deviation (σ) values for liquid PEG-400 + DMSO at different temperatures.

T/K	Par.*	A_o	A_1	A_2	A_3	A_4	σ
288.15		-9.237	5.450	-7.918	13.088		0.271
298.15	K_s^E	-9.922	7.449	-9.754	11.338		0.126
308.15		-10.794	10.231	-10.702	6.867		0.130
288.15		-12.872	7.619	-11.114	18.283		0.372
298.15	K_T^E	-13.665	10.123	-13.263	15.734		0.183
308.15		-14.665	13.650	-14.187	9.448		0.182
288.15		-4.883	2.911	-4.021	6.573		0.141
298.15	L_f^E	-5.201	3.947	-4.950	5.565		0.064
308.15		-5.614	5.390	-5.399	3.116		0.066
288.15		12.517	-11.399	-10.435	0.046	38.408	0.474
298.15	P_i^E	12.300	-11.202	0.828	-3.901	18.772	0.082
308.15		12.326	-12.213	9.205	-3.403	2.610	0.160
288.15		-0.818	0.487	-0.692	1.131		0.004
298.15	V_f^E	-0.859	0.640	-0.820	0.957		0.001
308.15		-0.913	0.856	-0.869	0.550		0.001

*Par. – parameter

The inspection of Fig. 2 reveals that the K_s^E is throughout negative in the given concentration range at 288.15 K. The overall negative trend of K_s^E indicates the presence of a hydrogen bonding between PEG-400 and DMSO.[54] Moreover, a close look at Fig. 2 shows that the magnitude of negative deviation is maximum around X_1~0.3. Furthermore, Fig. 2 displays that at temperatures 298.15 K and 308.15 K, a similar behaviour is observed for the PEG-400 and DMSO binary system. However, a slight increase in the negative value of K_s^E is obvious. This is likely because a rise in temperature enhances the kinetic energy of molecules, leading to the weakening of molecular interactions. The variations in K_T^E values with changes in mole fraction (X_1) and rise in temperature (Fig. 3) are similar to the variations observed for K_s^E values with such changes.

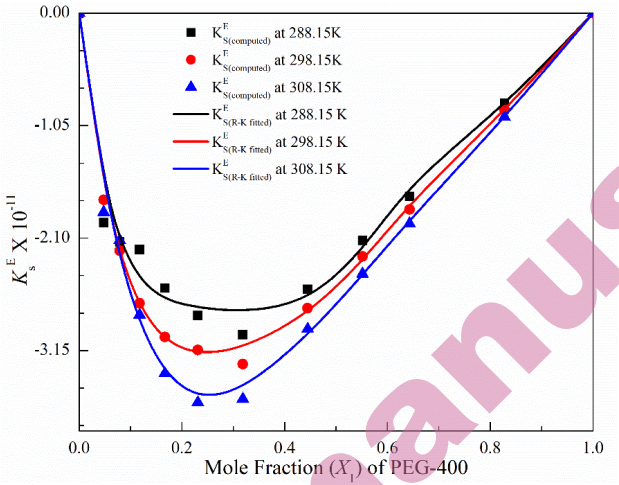

Fig. 2. Excess adiabatic compressibility (K_s^E) for PEG-400 + DMSO at different temperatures. The solid curves represents the Redlich – Kister equation fitting.

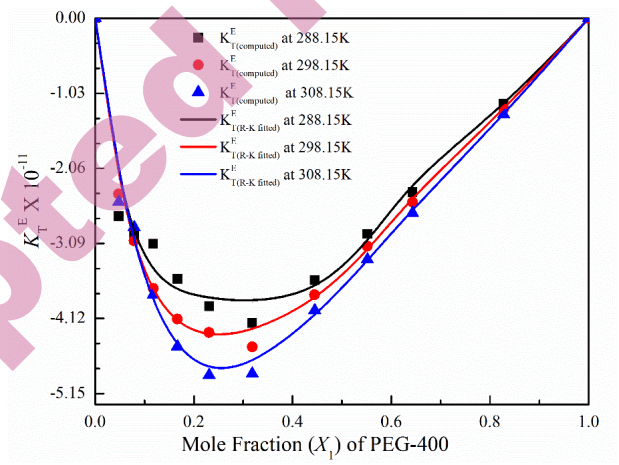

Fig. 3. Excess isothermal compressibility (K_T^E) for PEG-400 + DMSO at different temperatures. The solid curves represents the Redlich – Kister equation fitting.

Since intermolecular free length (L_f) and adiabatic compressibility (K_s) are directly related to each other, so with the increase in K_s values, an increase in L_f values is expected.[55] Table III reports that both K_s and L_f are decreasing with the rise in the mole fraction (X_1) of PEG-400. It is likely due to the quick uncoiling of the small-sized chain (Carbon atoms = 17) of PEG-400 in a highly polar aprotic organo-sulphur solvent DMSO (Dipole moment = 3.96D) due to dipole-induced dipole and hydrogen bonding interactions between solute and solvent molecules. The rise in the temperature from 298.15 K to 308.15 K for the mixture shows a slight increase in K_s and L_f values, this is as expected, as the enhancement of

thermal agitations in the system leads to more mobility of the molecules. The excess intermolecular free length (L_f^E) is directly linked with the weakening of intra-molecular interactions and the formation of H-bonding in the system.[54,55] The overall negative value of L_f^E for the mixture (Fig. 4) points to the presence of inter-molecular H-bonding in the system. The minimum value of L_f^E occurs around $X_1 \sim 0.3$, indicating the presence of the greatest strength of hydrogen bonding at that concentration. The order of strength of intermolecular interactions with the increase in temperature is $(L_f^E)_{288.15\ K} > (L_f^E)_{298.15\ K} > (L_f^E)_{308.15\ K}$.

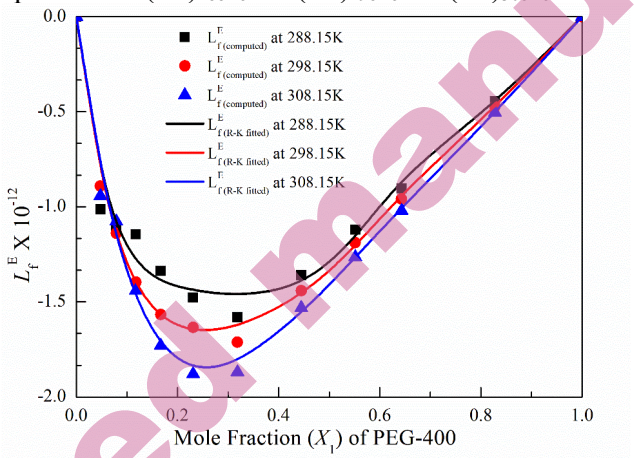

Fig. 4. Excess free length (L_f^E) for PEG-400 + DMSO at different temperatures. The solid curves represents the Redlich – Kister equation fitting.

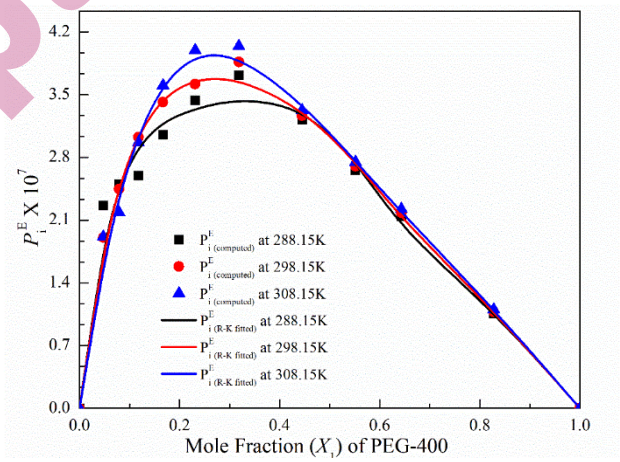

Fig. 5. Excess internal pressure (P_i^E) for PEG-400 + DMSO at different temperatures. The solid curves represent the Redlich–Kister equation fitting.

Internal pressure (P_i), the resultant of the molecules' attractive and repulsive interactions, is a parameter that is sensitive to all three types of interactions, viz., solute-solute (A-A), solute-solvent (A-B), and solvent-solvent (B-B) interactions, in a mixture.[56] The excess internal pressure (P_i^E) is also very sensitive to variations in the strength of the intermolecular interactions. Fig. 5 exhibits that P_i^E is positive over the entire mole fraction (X_1) range. It confirms that A-B interactions dominate over A-A and B-B interactions. Rao *et al.*,[57]reported that an increase in P_i values leads to a decrease in free volume (V_f). The negative values of V_f^E throughout the concentration range (Fig 6) point to the enhancement of compactness among the molecules of the mixture, confirming the existence of attractive interactions in the system.[58]Excess parameters viz. V_f^E, K_s^E, K_T^E, L_f^E, and P_i^E for the binary mixture studied here, are fitted with the Redlich-Kister polynomial equation, determined by the least-square regression method. Table IV reports the Redlich-Kister polynomial coefficients for the system in the temperature range of 288.15 K to 308.15 K. The low spread of standard deviation (σ) values points to the suitability of the Redlich-Kister polynomial equation for the system under study at all the temperatures investigated here.

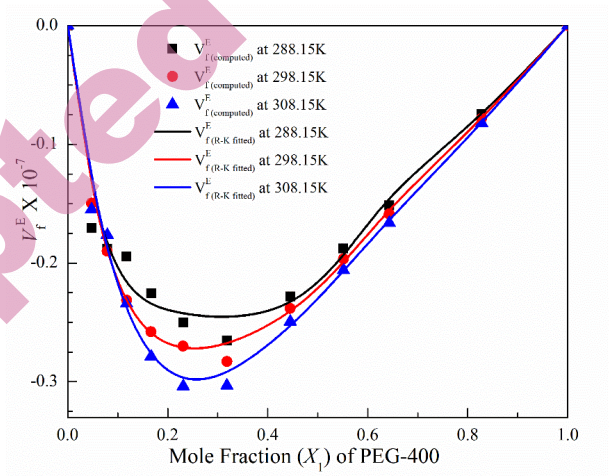

Fig. 6. Excess free volume (V_f^E) for PEG-400 + DMSO at different temperatures. The solid curves represent the Redlich – Kister equation fitting.

Partial and apparent molar volumes

For the given system of PEG-400 + DMSO, the partial molar volume ($\overline{V_1}$,$\overline{V_2}$), excess partial molar volume ($\bar{V}_1^E$,$\bar{V}_2^E$), apparent molar volume (V_{φ_1},V_{φ_2}) and apparent molar volume at infinite dilution ($\bar{V}_{\varphi_1}^{\infty}$,$\bar{V}_{\varphi_2}^{\infty}$) is computed and presented in Tables V and VI. Partial molar volumes and apparent molar volumes of solute and solvent are obtained using the standard procedure reported below (Eq. 16-19).[59,60]

Table V. Partial volume, excess partial molar volume and apparent molar volume for PEG-400(1) + DMSO (2) at different temperatures.

X_1	$\bar{V}_1$ ($cm^3.mol^{-1}$)	$\bar{V}_2$ ($cm^3.mol^{-1}$)	$\bar{V}_1^E$ ($cm^3.mol^{-1}$)	$\bar{V}_2^E$ ($cm^3.mol^{-1}$)	V_{φ_1} ($cm^3.mol^{-1}$)	V_{φ_2} ($cm^3.mol^{-1}$)
			288.15 K			
0	348.87(± 0.158)	70.66(± 0.032)	-5.015	0.000	-	70.66(± 0.032)
0.0477	349.79(± 0.157)	70.61(± 0.032)	-4.096	-0.046	348.87(± 0.157)	70.41(± 0.032)
0.0790	352.60(± 0.158)	70.40(± 0.032)	-1.290	-0.254	349.64(± 0.156)	70.29(± 0.031)
0.1178	354.62(± 0.158)	70.22(± 0.031)	0.738	-0.435	351.37(± 0.157)	70.32(± 0.031)
0.1668	352.46(± 0.157)	70.67(± 0.032)	-1.428	0.008	352.50(± 0.157)	70.38(± 0.031)
0.2310	351.97(± 0.156)	70.58(± 0.031)	-1.919	-0.075	351.72(± 0.156)	70.01(± 0.031)
0.3185	353.66(± 0.157)	70.10(± 0.031)	-0.230	-0.561	352.45(± 0.156)	69.99(± 0.031)
0.4448	353.75(± 0.157)	69.98(± 0.031)	-0.135	-0.680	352.90(± 0.156)	69.87(± 0.031)
0.5516	353.96(± 0.157)	69.82(± 0.031)	0.071	-0.838	353.28(± 0.157)	69.91(± 0.031)
0.6431	353.92(± 0.157)	69.87(± 0.031)	0.037	-0.786	353.49(± 0.157)	69.94(± 0.031)
0.8278	353.90(± 0.157)	69.95(± 0.031)	0.010	-0.708	353.75(± 0.157)	70.00(± 0.031)
1	353.89(± 0.157)	70.00(± 0.031)	0.000	-0.661	353.89(± 0.157)	-
			298.15 K			
0	351.51(± 0.160)	71.30(± 0.033)	-5.000	0.000	-	71.30(± 0.033)
0.0477	354.38(± 0.160)	71.16(± 0.032)	-2.130	-0.144	351.51(± 0.159)	71.05(± 0.032)
0.0790	357.41(± 0.162)	71.00(± 0.032)	0.901	-0.301	353.90(± 0.160)	71.08(± 0.032)
0.1178	357.86(± 0.162)	70.95(± 0.032)	1.345	-0.353	355.21(± 0.160)	71.13(± 0.032)
0.1668	356.53(± 0.161)	71.24(± 0.032)	0.022	-0.069	356.19(± 0.161)	71.24(± 0.032)
0.2310	354.47(± 0.159)	71.69(± 0.032)	-2.042	0.390	355.77(± 0.160)	71.08(± 0.032)
0.3185	355.28(± 0.159)	71.24(± 0.032)	-1.229	-0.066	355.14(± 0.159)	70.66(± 0.032)
0.4448	356.59(± 0.159)	70.61(± 0.032)	0.082	-0.692	355.73(± 0.159)	70.68(± 0.032)
0.5516	356.61(± 0.159)	70.61(± 0.032)	0.099	-0.696	356.04(± 0.159)	70.73(± 0.032)
0.6431	356.56(± 0.159)	70.68(± 0.032)	0.051	-0.624	356.22(± 0.159)	70.77(± 0.032)
0.8278	356.52(± 0.159)	70.79(± 0.032)	0.014	-0.515	356.42(± 0.159)	70.86(± 0.032)
1	356.51(± 0.159)	70.86(± 0.032)	0.000	-0.449	356.51(± 0.159)	-
			308.15 K			
0	355.86(± 0.164)	71.86(± 0.033)	-3.292	0.000	-	71.86(± 0.033)
0.0477	359.39(± 0.164)	71.69(± 0.033)	0.236	-0.177	355.86(± 0.163)	71.70(± 0.033)
0.0790	361.29(± 0.165)	71.65(± 0.033)	2.137	-0.214	358.80(± 0.164)	71.83(± 0.033)
0.1178	360.56(± 0.164)	71.67(± 0.033)	1.405	-0.193	359.11(± 0.164)	71.86(± 0.033)
0.1668	359.06(± 0.163)	72.03(± 0.033)	-0.094	0.166	359.89(± 0.164)	72.01(± 0.033)
0.2310	356.96(± 0.162)	72.42(± 0.033)	-2.195	0.558	358.82(± 0.163)	71.76(± 0.033)
0.3185	358.03(± 0.162)	71.97(± 0.032)	-1.119	0.104	358.26(± 0.162)	71.44(± 0.032)
0.4448	359.05(± 0.162)	71.41(± 0.032)	-0.098	-0.452	358.49(± 0.161)	71.33(± 0.032)
0.5516	359.26(± 0.162)	71.25(± 0.032)	0.112	-0.609	358.77(± 0.161)	71.39(± 0.032)
0.6431	359.21(± 0.162)	71.34(± 0.032)	0.058	-0.527	358.92(± 0.161)	71.44(± 0.032)
0.8278	359.17(± 0.162)	71.46(± 0.032)	0.015	-0.404	359.08(± 0.161)	71.53(± 0.032)
1	359.15(± 0.162)	71.53(± 0.032)	0.000	-0.330	359.15(± 0.161)	-

[a]The standard uncertainties (u) are $u(T)$= 0.01 K, $u(d)$= 0.5 kgm^{-3}, $u(U)$= 1.0 ms^{-1} and $U(x_1)$= 0.0001 kg/mol.

Table VI. Molar volume and apparent molar volume at infinite dilution for PEG-400(1) + DMSO (2) at different temperatures.

T/K	V_1 (cm^3mol^{-1})	V_2 (cm^3mol^{-1})	$\bar{V}_{\varphi_1}^{\infty}$ (cm^3mol^{-1})	$\bar{V}_{\varphi_2}^{\infty}$ (cm^3mol^{-1})
288.15	353.89	70.66	350.44	70.40
298.15	356.51	71.30	354.11	71.16
308.15	359.15	71.86	358.22	71.85

$$\bar{V}_1 = V + (1 - X_1)\frac{\partial V}{\partial X_1} \quad (16)$$

$$\bar{V}_2 = V + (1 - X_2)\frac{\partial V}{\partial X_2} \quad (17)$$

$$V_{\varphi_1} = V_1 + \frac{V_m^E}{X_1} \quad (18)$$

$$V_{\varphi_2} = V_2 + \frac{V_m^E}{X_2} \quad (19)$$

Here, V_m^E is the molar excess volume, ($\bar{V}_1$, $\bar{V}_2$) and (V_{φ_1}, V_{φ_2}) are the molar and apparent molar volumes of PEG-400 (1) and DMSO (2) respectively. The values of (V_{φ_1}, V_{φ_2}) at infinite dilution ($\bar{V}_{\varphi_1}^{\infty}$, $\bar{V}_{\varphi_2}^{\infty}$) are determined using analytical extrapolation methods. In this approach, $\bar{V}_{\varphi_1}^{\infty}$ is obtained by taking V_{φ_1} to X_1=0 (X_2=1) and $\bar{V}_{\varphi_2}^{\infty}$ is obtained by taking the V_{φ_2} to X_2=0 (X_1=1).

The portray of Table V indicate that in general, the excess partial volumes ($\bar{V}_1^E$,$\bar{V}_2^E$) are negative at all temperatures. It is well mentioned in literature that, the negative values of $\bar{V}_1^E$ and $\bar{V}_2^E$ is an indicative of intermolecular interaction by hydrogen bonding or due to geometrical fitting of one component into another.[61]These findings are in agreement with the results arrived earlier for the given system PEG-400 + DMSO. The apparent molar volume at infinite dilution ($\bar{V}_{\varphi_1}^{\infty}$, $\bar{V}_{\varphi_2}^{\infty}$) is an important property to access the solute-solvent interaction of the liquid mixtures. At infinite dilution, the apparent molar volume only depends upon the solute-solvent interaction, and the contribution of solute-solute interactions disappears in the mixture; furthermore, at infinite dilution, solute-solvent interaction becomes independent of the composition of the mixture.[61] The apparent molar volume for solute and solvent at different temperatures are reported in Table VI. The inspection of Table VI reveals that the apparent molar volume at infinite dilution ($\bar{V}_{\varphi_1}^{\infty}$, $\bar{V}_{\varphi_2}^{\infty}$) for PEG-400 and DMSO is less than that of pure molar volume (V_1, V_2), which confirms the solute-solvent interactions in the system.[60] Furthermore, the difference of ($\bar{V}_{\varphi_1}^{\infty}$, $\bar{V}_{\varphi_2}^{\infty}$) with ($V_1$, V_2) decreases with temperature, which indicates that the solute-solvent interactions get weakens with the rise in temperature.

Theoretical estimation of ultrasonic velocity of the mixture

Using various standard relations such as the ideal mixing relation (IMR), Nomoto relation (NR), impedance dependence relation (IDR), Van Deal-Vangeel relation (VVR), and Junjie relation (JR), and Schaaff's Collision Factor Theory

(CFT), ultrasonic velocities in the PEG-400 + DMSO mixture have been determined. The experimentally measured values of ultrasonic velocity (U^*) along with theoretically predicted U_{IM}, U_N, U_Z, U_V, U_J, and U_{CFT} values, at T = 288.15, 298.15, and 308.15 K, for the binary mixture under study are reported in Table VII. It is observed that U_N and U_J are well matches with U^*, whereas U_{IM}, U_Z, and U_{CFT} are showing a reasonable agreement with the experimental values. However, U_V values show a large departure from experimental values. Thereby, the Van Deal-Vangeel relation (VVR) fails to determine the ultrasonic velocity values in the given temperature and concentration range for the system. It is likely due to the large difference in size of the molecules of PEG-400 and DMSO. To have a better understanding of the compatibility of these relations to predict the ultrasonic velocity in the given concentration and temperature range for the system, the absolute percentage deviation (APD) values were determined. These values are presented in Table VIII. It is worth noting here that, APD values for U_N (NR) and U_J (JR) are < 1%, ~ 2% for U_{IM} (IMR) and U_Z (IDR), and ~ 18% for U_V (VVR) at all the working temperatures. Moreover, the APD value for CFT is < 1% at 308.15 K, 3.0% at 288.15 K, and 1.1 % at 298.15 K. Thus, it can be concluded that except VVR, the other five relations, investigated here, can be successfully employed to predict the ultrasonic velocity for the system, in the given concentration range and at all working temperatures.

Table VII. Experimental (U^*) and calculated ultrasonic velocity using different mixing rules for PEG-400 + DMSO at different temperatures

X_1	U^*	U_{IM}	U_N	U_Z	U_V	U_J	U_{CFT}
T = 288.15 K							
0	1524	1524	1524	1524	1524	1524	1513
0.0477	1564	1529	1545	1529	1422	1543	1529
0.0790	1569	1533	1555	1533	1370	1553	1536
0.1178	1574	1537	1566	1537	1317	1563	1541
0.1668	1587	1542	1576	1542	1264	1574	1545
0.2310	1598	1549	1587	1549	1213	1584	1553
0.3185	1613	1558	1597	1558	1169	1595	1557
0.4448	1618	1571	1608	1572	1140	1606	1560
0.5516	1621	1582	1614	1583	1144	1613	1561
0.6431	1623	1592	1619	1592	1168	1618	1561
0.8278	1627	1611	1625	1612	1296	1625	1561
1	1629	1629	1629	1629	1629	1629	1560
T = 298.15 K							
0	1490	1490	1490	1490	1490	1490	1510
0.0477	1523	1495	1511	1495	1390	1509	1527
0.0790	1534	1498	1521	1499	1339	1519	1532
0.1178	1548	1502	1532	1503	1287	1529	1536
0.1668	1559	1508	1542	1508	1236	1539	1541
0.2310	1568	1514	1553	1515	1186	1550	1547

X_1	U^*	U_{IM}	U_N	U_Z	U_V	U_J	U_{CFT}
0.3185	1579	1524	1563	1524	1143	1561	1554
0.4448	1584	1537	1574	1537	1115	1572	1557
0.5516	1587	1548	1580	1549	1119	1579	1558
0.6431	1589	1558	1584	1558	1142	1583	1559
0.8278	1592	1577	1591	1577	1268	1590	1559
1	1595	1595	1595	1595	1595	1595	1558
T = 308.15 K							
0	1457	1457	1457	1457	1457	1457	1507
0.0477	1489	1462	1477	1462	1359	1475	1523
0.0790	1497	1465	1488	1465	1309	1485	1526
0.1178	1513	1469	1498	1469	1258	1495	1532
0.1668	1529	1474	1509	1474	1208	1506	1536
0.2310	1540	1481	1519	1481	1160	1516	1544
0.3185	1548	1490	1530	1491	1117	1527	1551
0.4448	1550	1503	1540	1504	1090	1539	1555
0.5516	1553	1515	1547	1515	1094	1545	1556
0.6431	1555	1524	1551	1525	1117	1550	1557
0.8278	1559	1544	1558	1544	1240	1557	1557
1	1562	1562	1562	1562	1562	1562	1557

Table VIII. Absolute Percentage Deviation (APD) for ultrasonic velocity mixing rules applied on PEG-400 + DMSO at different temperatures.

T (K)	$\%U_{IM}$	$\%U_N$	$\%U_Z$	$\%U_V$	$\%U_J$	$\%U_{CFT}$
288.15	2.0	0.5	2.0	18.1	0.6	3.0
298.15	2.1	0.6	2.1	18.2	0.7	1.1
308.15	2.2	0.6	2.2	18.3	0.8	-0.8

UV-Vis Spectra

The UV-Vis spectra of PEG-400 with DMSO is presented in Fig 7. A close look at Fig. 7 reveals that the absorption peak of PEG-400 is shifted from 247 nm to 253 nm as DMSO concentration increases in the mixture, which indicates the possibility of hydrogen bonding between the hydrogen of the hydroxyl group of PEG-400 and the free lone pair of oxygen atom of DMSO i.e. $(CH_3)_2S{=}O{---}H{-}(OCH_2 - CH_2 - O)_{PEG}{-}\ H{---}O{=}S(CH_3)_2$.[35] It can be attributed to the $n \rightarrow \pi^*$ electronic transition of the unshaped electronic pair of oxygen atoms in DMSO.

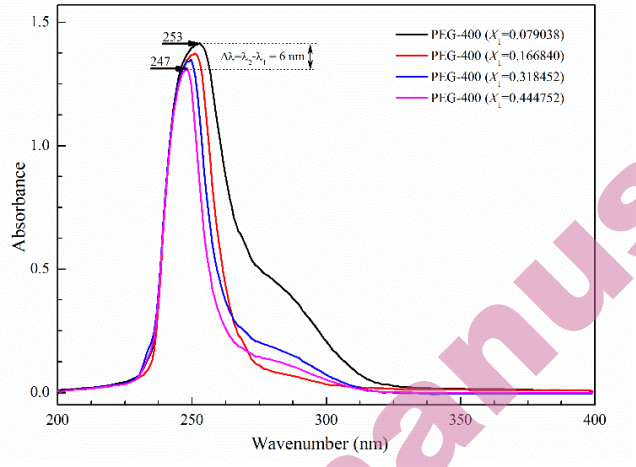

Fig. 7. UV-vis spectra of PEG-400 + DMSO at increasing concentrations of DMSO.

FTIR Spectra

The FTIR spectra of pure DMSO, pure PEG-400, and their binary mixture are presented in Fig 8(a), Fig. 8(b), and Fig. 8(c-e) respectively. The perusal of spectra of pure DMSO [Fig 8(a)] indicates a peak at wave number 3430.65cm^{-1}, which is indicative of O-H stretching.

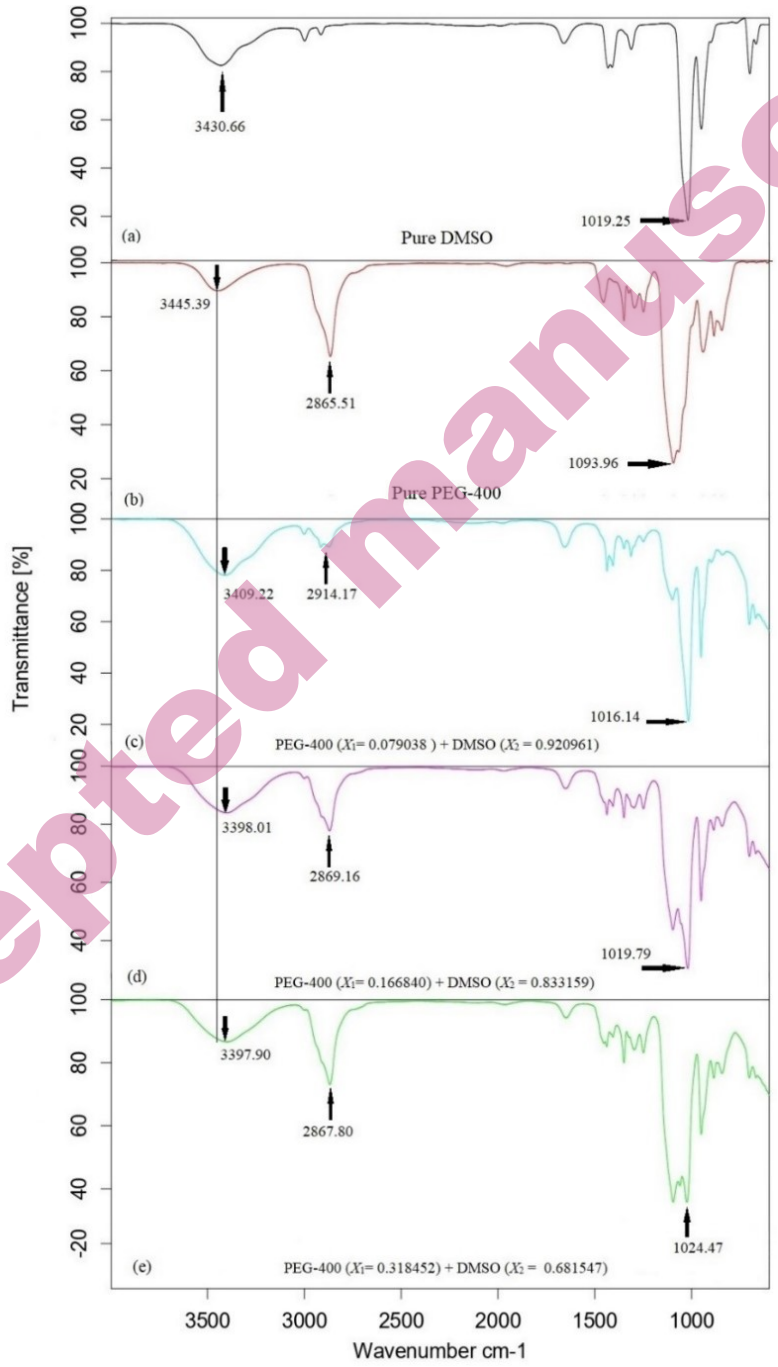

Fig. 8. FTIR spectra of pure PEG-400, pure DMSO and PEG-400 + DMSO at different concentrations.

Whereas a peak at 1019.25 cm^{-1} depicts C-S stretching vibrations of molecules. The close look of Fig 8 also infers a considerable shift (~ 36 – 48 cm^{-1}) as well as broadening in the 3445.39 cm^{-1} peak with the change in concentration DSMO in the mixtures [Fig 8 (c-e)]. This is most likely due to the breaking of the intra-molecular interactions of PEG-400 and the formation of intermolecular H-bonding between PEG-400 and DMSO molecules. Moreover, when the amount of PEG-400 (solute) is increased in the mixture the peak at wave number 1019.25 cm^{-1} of pure DMSO [Fig. 8(a)] splits into two peaks. It indicates the presence of intermolecular interactions and the formation of a dimmer in the system.[19] The conclusions based on FTIR spectra of the binary mixtures supplement the findings arrived at by using the ultrasonic technique for the system.

CONCLUSION

New experimental values of ultrasonic velocity and density have been determined for a polymer mixture of PEG-400 and DMSO at T = 288.15 K, 298.15 K, and 308.15 K. Based on ultrasonic velocity and density, some important physical parameters and their excess values are also computed. The current investigation confirms the intermolecular H-bonding between PEG-400 and DMSO molecules. The spectroscopic analysis of the given system also confirms the presence of intermolecular H-bonding between PEG-400 and DMSO. Additionally, the validity of various mixing rules for ultrasonic velocity has also been tested for given mixtures at different temperatures. It can be concluded that out of six mixing rules, the Nomoto relation and the Junjie relation are found to be best suited for the given mixture. Overall, this insightful analysis of the given mixtures can be useful in industry for solvent selection, design, extraction, and separation processes.

SUPPLEMENTARY MATERIAL

Additional data are available electronically at the pages of journal website: https://www.shd-pub.org.rs/index.php/JSCS/article/view/12720, or from the corresponding author on request.

И З В О Д

ИСПИТИВАЊЕ МОЛЕКУЛАРНИХ ИНТЕРАКЦИЈА БИНАРНИХ МЕШАВИНА ПЕГ-400 И ДМСО НА РАЗЛИЧИТИМ ТЕМПЕРАТУРАМА УЛТРАЗВУКОМ И СПЕКТРОСКОПСКОПИЈОМ ИСТРАГЕ

MONIKA DHIMAN[1], ARUN UPMANYU[1*], DEVINDER PAL SINGH[2], KAILASH CHANDRA JUGLAN[3]

[1]Chitkara University Institute of Engineering and Technology, Chitkara University, Punjab, 140401, India, [2]Acoustics Research Center, Mississauga, L5A 1Y7, Ontario, Canada, and [3]Department of Physics, Lovely Faculty of Technology and Sciences, Lovely Professional University, Punjab, India

У раду су приказани резулати мерења ултразвучне брзина и густине бинарне смеше Поли(етилен-гликола) (PEG)-400 и диметил-сулфоксида (DMSO), при различитим концентрацијама и различитим температурама (T = 288,15 K, 298.15 K и 308.15 K), који су додатно искоришћени за утврђивање неколико физичких параметара као што су адиабатичка и изотермална компресија, интермолекуларна слободна дужина, унутрашњи притисак и слободна запремина. Вишак вредности ових параметара је такође израчунат и фитован са Redlich-Kister (R-K) полиномном једначином. Природа , тип и јачина интермолекуларних интеракција присутних у PEG-400 + DMSO смеши објашњени су на основу знака и величине вишка вредности. Поред тога одређени су парцијална запремина, вишак парцијалне запремине, моларна запремина при бесконачном разблаживању да би се испитале интеракције растворак-растварач. Разна правила мешања као што су идеално правило мешања (U_{im}), Nomoto (U_N), однос зависности од импедансе (U_Z), Junjie (U_J), Van Deal-Vangeel (U_V) и теорија фактора судара (U_{CFT}) су употребљена за израчунавање ултразвучне брзине и упоређени са експерименталном. Nomoto и Junjie једначие набоље описују смешу. Систем је такође испитан коришћењем FTIR и UV-Vis спектроскопскопијом Промена интензитета и померање пика у FTIR и UV-Vis спектру PEG-400 + DMSO смеше су потврдиле водоничне везе у систему.

(Примљено 7. децембра 2023; ревидирано 22. јануара 2024; прихваћено 2. јуна 2024.)

REFERENCES

1. P. Malik, G. Chauhan, P. Kumar, A. Deep, *Liq. Cryst.* **49** (2022) 2008–2018 (https://doi.org/10.1080/02678292.2022.2094006)
2. P. Kumar, V. Sharma, P. Malik, & K. K. Raina, *J. Mol. Struct.* **1196** (2019) 866–873 (https://doi.org/10.1016/j.molstruc.2019.06.045)
3. S. Tian, Y. Hou, W. Wu, S. Ren, J. Qian, *J. Hazard. Mater.* **278** (2014) 409–416 (https://doi.org/10.1016/j.jhazmat.2014.06.037)
4. K. T. Lee, A. R. Mohamed, S. Bhatia, K. H. Chu. *J. Chem. Eng.* **114 (**2005) 171-177 (https://doi.org/10.1016/j.cej.2005.08.020)
5. T. Zhao, J. Zhang, B. Guo, F. Zhang, F. Sha, X. Xie, X. Wei, *J. Mol. Liq.* **207** (2015) 315–322 (https://doi.org/10.1016/j.molliq.2015.04.001)
6. K. Zhang, J. Yang, X. Yu, J. Zhang, X. Wei, *J. Chem. Eng. Data* **56** (2011) 3083–3088 (https://doi.org/10.1021/je200148u)
7. J. Rodríguez-Sevilla, M. Álvarez, G. Limiñana, M. C. Díaz, *J. Chem. Eng. Data* **47** (2002) 1339–1345 (https://doi.org/10.1021/je015538e)
8. D. Nagel, R. de Kermadec, H. G. Lintz, C. Roizard, F. Lapicque. *Chem. Eng. Sci.* **57** (2002) 4883-4893 (https://doi.org/10.1016/S0009-2509(02)00283-X)
9. F. Han, J. Zhang, G. Chen, X. Wei, *J. Chem. Eng. Data* **53** (2008) 2598–2601 (https://doi.org/10.1021/je800464t)
10. S. Trivedi, C. Bhanot, S. Pandey, *J. Chem. Thermodyn.* **42** (2010) 1367–1371 (https://doi.org/10.1016/j.jct.2010.06.001)
11. A. Upmanyu, M. Dhiman, D. P. Singh, H. Kumar, *J. Mol. Liq.* **334** (2021) 115939 (https://doi.org/10.1016/j.molliq.2021.115939)
12. B. V. Kumar Naidu, K. C. Rao, M. C. S. Subha, *J. Chem. Eng. Data* **47** (2002) 379–382 (https://doi.org/10.1021/je0101395)
13. M. Dhiman, K. Singh, J. Kaushal, A. Upmanyu, D. P. Singh, *Acta Acust. united with Acust.* **105** (2019) 743–752 (https://doi.org/10.3813/AAA.919354)

14. M. Rani, S. Gahlyan, A. Gaur, S. Maken, *Chinese J. Chem. Eng.* **23** (2015) 689–698 (https://doi.org/10.1016/j.cjche.2014.12.003)
15. P. Kaur, N. Chakraborty, K. C. Juglan, H. Kumar, *J. Mol. Liq.* **315** (2020) 113763 (https://doi.org/10.1016/j.molliq.2020.113763)
16. D. P. Gupta, A. Upmanyu, M. Dhiman, D. P. Singh, *Estimation of ultrasonic velocity and viscosity of polymer solutions of HTPB+ chlorobenzene at different temperatures*. in *AIP Conf. Proc.*, AIP Publishing, 2022 (https://doi.org/10.1063/5.0080974)
17. A. Ali, A. K. Nain, V. K. Sharma, S. Ahmad, *Phys. Chem. Liq.* **42** (2004) 375–383 (https://doi.org/10.1080/00319100410001679882)
18. M. Umadevi, R. Kesavasamy, K. Rathina, R. Mahalakshmi. *J. Mol. Liq.* **219** (2016) 820-828 (https://doi.org/10.1016/j.molliq.2016.03.085)
19. L. Ma, F. Sha, X. Qiao, Q. Li, J. Zhang, *Chinese J. Chem. Eng.* **25** (2017) 1249–1255 (https://doi.org/10.1016/j.cjche.2017.01.001)
20. G. Arivazhagan, A. Elangovan, R. Shanmugam, R. Vijayalakshmi, N. K. Karthick, *J. Mol. Liq.* **214** (2016) 357–363 (https://doi.org/10.1016/j.molliq.2015.10.062)
21. L. M. Madikizela, P. S. Mdluli, L. Chimuka, *React. Funct. Polym.* **103** (2016) 33–43 (https://doi.org/10.1016/j.reactfunctpolym.2016.03.017)
22. T. S. Krishna, K. Raju, M. Gowrisankar, A. K. Nain, B. Munibhadrayya, *J. Mol. Liq.* **216** (2016) 484–495 (https://doi.org/10.1016/j.molliq.2016.01.085)
23. A. Awasthi, J. P. Shukla, *Ultrasonics* **41** (2003) 477–486 (https://doi.org/10.1016/S0041-624X(03)00127-6)
24. P. Malik, S. Kumar, Khushboo, A. Upmanyu, P. Kumar, P. Malik, *Liq. Cryst.* **49** (2022) 1604–1611 (https://doi.org/10.1080/02678292.2022.2102684)
25. O. E.-A. A. Adam, A. A. Hassan, *Phys. Chem. Liq.* **56** (2018) 55–68 (https://doi.org/10.1080/00319104.2017.1292424)
26. N. Chaudhary, A. Kumar Nain, *Phys. Chem. Liq.* **58** (2020) 736–759 (https://doi.org/10.1080/00319104.2019.1636378)
27. M. T. Zafarani-Moattar, N. Tohidifar, *J. Chem. Eng. Data* **51** (2006) 1769–1774 (https://doi.org/10.1021/je0601715)
28. M. T. Zafarani-Moattar, N. Tohidifar, *J. Chem. Eng. Data* **53** (2008) 785–793 (https://doi.org/10.1021/je700651e)
29. H. Patel, Z. S. Vaid, U. U. More, S. P. Ijardar, N. I. Malek, *J. Chem. Thermodyn.* **99** (2016) 40–53 (https://doi.org/10.1016/j.jct.2016.02.025)
30. F. M. Sannaningannavar, B. S. Navati, N. H. Ayachit, *J. Therm. Anal. Calorim.* **112** (2013) 1573–1578 (https://doi.org/10.1007/s10973-012-2724-5)
31. J. G. Baragi, M. I. Aralaguppi, T. M. Aminabhavi, M. Y. Kariduraganavar, A. S. Kittur, *J. Chem. Eng. Data* **50** (2005) 910–916 (https://doi.org/10.1021/je049610v)
32. S. Baluja, R. M. Talaviya, *J. Chem. Eng. Data* **61** (2016) 1431–1440 (https://doi.org/10.1021/acs.jced.5b00627)
33. V. K. Syal, S. Chauhan, R. Gautam, *Ultrason.* **36** (1998) 619-623 (https://doi.org/10.1016/S0041-624X(97)00104-2)
34. D. Keshapolla, R. L. Gardas, *Fluid Phase Equilib.* **383** (2014) 32–42 (https://doi.org/10.1016/j.fluid.2014.09.022)
35. T. Zhao, Q. Xu, J. Xiao, X. Wei, *J. Chem. Eng. Data* **60** (2015) 2135–2145 (https://doi.org/10.1021/acs.jced.5b00209)
36. A. Ali, F. Nabi, *J. Dispers. Sci. Technol.* **31** (2010) 1326–1334 (https://doi.org/10.1080/01932690903227469)

37. H. Wang, W. Liu, J. Huang, *J. Chem. Thermodyn.* **36** (2004) 743–752 (https://doi.org/10.1016/j.jct.2004.04.004)
38. R. K. Shukla, S. N. Dixit, P. Jain, P. Mishra, S. Sharma, *Orbital-The Electron. J. Chem.* **2** (2011) 356–364 (https://periodicos.ufms.br/index.php/orbital/article/view/17980/12479)
39. J. C. De La Torre, *Ann. N. Y. Acad. Sci.* **411** (1983) 293–308 (https://doi.org/10.1111/j.1749-6632.1983.tb47311.x)
40. M. T. Zafarani-Moattar, H. Shekaari, *J. Chem. Thermodyn.* **38** (2006) 624–633 (https://doi.org/10.1016/j.jct.2005.07.018)
41. A. Ali, A. K. Nain, D. Chand, R. Ahmad, *Bull. Chem. Soc. Jpn.* **79** (2006) 702–710 (https://doi.org/10.1246/bcsj.79.702)
42. J. Krakowiak, D. Bobicz, W. Grzybkowski, *J. Mol. Liq.* **88** (2000) 197–207 (https://doi.org/10.1016/S0167-7322(00)00154-9)
43. H. Shekaari, M. T. Zafarani-Moattar, *Int. J. Thermophys.* **29** (2008) 534–545 (https://doi.org/10.1007/s10765-008-0395-z)
44. S. R. Dandwate, S. B. Deshmukh, *J. Curr. Pharma Res.* **10** (2020) 3716–3723 (ISSN-2230-7842 CODEN-CPRUE6, www.jcpronline.in/)
45. U. R. Kapadi, S. K. Chavan, O. S. Yemul, *J. Chem. Eng. Data* **42** (1997) 548–550 (https://doi.org/10.1021/je960216+)
46. G. Ritzoulis, *Can. J. Chem.* **67** (1989) 1105–1108 (https://doi.org/10.1139/v89-166)
47. M. A. Saleh, O. Ahmed, M. S. Ahmed, *J. Mol. Liq.* **115** (2004) 41–47 (https://doi.org/10.1016/j.molliq.2003.12.021)
48. S. B. Aznarez, L. Mussari, M. A. Postigo, *J. Chem. Eng. Data* **38** (1993) 270–273 (https://doi.org/10.1021/je00010a022)
49. S. Parveen, D. Shukla, S. Singh, K. P. Singh, M. Gupta, J. P. Shukla, *Appl. Acoust.* **70** (2009) 507–513 (https://doi.org/10.1016/j.apacoust.2008.05.008)
50. B. Nagarjun, A. V. Sarma, G. R. Rao, C. Rambabu. *J. Thermodyn.* **2013** (2013) 285796 (https://doi.org/10.1155/2013/285796)
51. A. Zhu, J. Wang, R. Liu, *J. Chem. Thermodyn.* **43** (2011) 796–799 (https://doi.org/10.1016/j.jct.2010.12.027)
52. A. Ali, A. K. Nain, V. K. Sharma, S. Ahmad, *Phys. Chem. Liq.* **42** (2004) 375–383 (https://doi.org/10.1080/00319100410001679882)
53. P. R. Bevington, D. K. Robinson. Data reduction and error analysis for the physical sciences McGraw-Hill. New York. **19692** (1969) 235-242 (ISBN 0-07-247227-8)
54. M. Dhiman, K. Singh, D. P. Gupta, D. P. Singh, A. Upmanyu, *Study of excess acoustical and thermo-dynamical parameters of binary solutions of polypropylene glycol-400 and n-alkanols at 303 K*. in *AIP Conf. Proc.*, AIP Publishing, 2020 (https://doi.org/10.1063/5.0001107)
55. B. Thanuja, G. Nithya, C. C. Kanagam, *Ultrason. Sonochem.* **19** (2012) 1213–1220 (https://doi.org/10.1016/j.ultsonch.2012.03.006)
56. A. Awasthi, A. Awasthi. *Phys. Chem. Liq.* **51** (2013) 112-123 (https://doi.org/10.1080/00319104.2012.690569)
57. G. V Rao, A. V. Sarma, D. Ramachandran, C. Rambabu, *Ind. J. Pure App. Phys.* **42** (2004) 820–826 (http://nopr.niscpr.res.in/handle/123456789/8851)
58. S. F. Babavali, D. Punyaseshudu, K. Narendra, C. S. Yesaswi, C. Srinivasu, *J. Mol. Liq.* **224** (2016) 47–52 (https://doi.org/10.1016/j.molliq.2016.09.079)
59. M. Dhiman, A. Upmanyu, P. Kumar, D. P. Singh, *Karbala Int. J. Mod. Sci.* **8** (2022) 703–717 (https://doi.org/10.33640/2405-609X.3270)

60. S. Gahlyan, M. Rani, S. Maken, *J. Mol. Liq.* **199** (2014) 42–50 (https://doi.org/10.1016/j.molliq.2014.08.011)
61. H. E. Hoga, R. B. Torres, *J. Chem. Thermodyn.* **43** (2011) 1104–1134 (https://doi.org/10.1016/j.jct.2011.02.018).